

A k -Space Method for Large-Scale Models of Wave Propagation in Tissue

T. Douglas Mast, *Member, IEEE*, Laurent P. Souriau, D.-L. Donald Liu, *Member, IEEE*, Makoto Tabei, *Member, IEEE*, Adrian I. Nachman, and Robert C. Waag, *Fellow, IEEE*

Abstract—Large-scale simulation of ultrasonic pulse propagation in inhomogeneous tissue is important for the study of ultrasound-tissue interaction as well as for development of new imaging methods. Typical scales of interest span hundreds of wavelengths; most current two-dimensional methods, such as finite-difference and finite-element methods, are unable to compute propagation on this scale with the efficiency needed for imaging studies. Furthermore, for most available methods of simulating ultrasonic propagation, large-scale, three-dimensional computations of ultrasonic scattering are infeasible. Some of these difficulties have been overcome by previous pseudospectral and k -space methods, which allow substantial portions of the necessary computations to be executed using fast Fourier transforms. This paper presents a simplified derivation of the k -space method for a medium of variable sound speed and density; the derivation clearly shows the relationship of this k -space method to both past k -space methods and pseudospectral methods. In the present method, the spatial differential equations are solved by a simple Fourier transform method, and temporal iteration is performed using a k - t space propagator. The temporal iteration procedure is shown to be exact for homogeneous media, unconditionally stable for “slow” ($c(x) \leq c_0$) media, and highly accurate for general weakly scattering media. The applicability of the k -space method to large-scale soft tissue modeling is shown by simulating two-dimensional propagation of an incident plane wave through several tissue-mimicking cylinders as well as a model chest wall cross section. A three-dimensional implementation of the k -space method is also employed for the example problem of propagation through a tissue-mimicking sphere. Numerical results indicate that the k -space method is accurate for large-scale soft tissue computations with much greater efficiency than that of an analogous leapfrog pseudospectral method or a 2-4 finite difference time-domain method. However, numerical results also indicate that the k -space method is less accurate than the finite-difference method for a high contrast scatterer with bone-like properties, although qualitative results can still be obtained by the k -space method with high efficiency. Possible extensions to the method, including representa-

tion of absorption effects, absorbing boundary conditions, elastic-wave propagation, and acoustic nonlinearity, are discussed.

I. INTRODUCTION

COMPUTATION of a scattered acoustic field, given an incident wavefield and complete specification of an inhomogeneous medium, is known as the forward scattering problem. Numerical solution of the forward scattering problem is central to many aspects of ultrasonic imaging, including inverse scattering methods, numerical studies of wavefront distortion, and development of new methods for adaptive focusing. Most methods for numerical solution of the forward scattering problem fall into one of three categories: finite difference methods, finite element methods, and spectral methods.

Finite difference and finite element methods are known as local because the wave propagation equations of interest are solved at each point based only on conditions at nearby points. In contrast, spectral methods, such as the k -space method [1]–[7] and the pseudospectral approach [8]–[14], are called global because information from the entire wavefield is employed to solve the wave propagation equations at each point. In part because of their global nature, spectral methods can be more accurate than local methods—for instance, pseudospectral methods applied to periodic problems have been shown to be equivalent to finite difference methods of infinite order [12].

Spectral methods also have considerable advantages for large-scale forward solvers because the required storage and the number of operations per iteration can be dramatically reduced compared with local methods. This advantage occurs principally because spectral methods can allow computations to be performed on coarser grids while maintaining accuracy. For example, finite element methods and high-order finite difference methods typically require grid spacings on the order of 10 points per minimum wavelength; second-order finite difference methods can require 20 points per wavelength [10]. Spectral methods, in theory, require only two points per wavelength (spatial Nyquist sampling), although for computations of propagation in inhomogeneous media, greater accuracy is achieved with grid spacings on the order of four points per wavelength [10], [11], [14].

This report addresses the problem of large-scale ultrasonic wave propagation in biological media, such as human

Manuscript received February 26, 1999; accepted August 9, 2000. This research was funded by NIH Grants DK 45533, HL 50855, CA 74050, and 1R29CA81688; US Army Grant DAMD-17-98-1-8141; DARPA Grant N00014-96-0749; and the University of Rochester Diagnostic Ultrasound Research Laboratory Industrial Associates.

T. D. Mast is with the Applied Research Laboratory, The Pennsylvania State University, University Park, PA 16802 (e-mail: mast@sabine.acs.psu.edu).

D.-L. Donald Liu is with the Ultrasound Group, Siemens Medical Systems, Issaquah, WA 98027.

L. P. Souriau, M. Tabei, and R. C. Waag are with the Department of Electrical and Computer Engineering, University of Rochester, Rochester, NY 14627. R. C. Waag is also with the Department of Radiology.

A. I. Nachman is with the Department of Mathematics, University of Rochester, Rochester, NY 14627.

tissue. For problems of interest in medical ultrasound, domain sizes can often exceed the capabilities of conventional forward solvers. For example, one computation of realistic scale would be the simulated propagation of a pulse with an upper bandwidth limit of 5 MHz in a volume of dimensions 30 mm on each side and a nominal sound speed of 1.5 mm/ μ s, so that the minimum wavelength is 0.3 mm. For this computation, a second-order finite difference method (using 20 points per wavelength) would require a three-dimensional grid containing 8×10^9 nodes; a finite element or fourth-order finite difference method (using 10 points per wavelength) would require 1×10^9 nodes; and a spectral method (using four points per wavelength) would require 6.4×10^7 nodes. Because a grid of 6.4×10^7 single precision complex numbers requires storage of 512 megabytes, only spectral methods are feasible for realistic three-dimensional computations on present-day computers that typically have a maximum random-access memory storage of several gigabytes. The efficiency provided by fast Fourier transform implementations of spectral algorithms is a further reason why spectral methods are a practical approach to large-scale and three-dimensional computations of ultrasonic wave propagation.

Previous spectral approaches have included pseudospectral methods, in which spatial derivatives are evaluated globally by Fourier transformation and wavefields are advanced in time using various numerical integration techniques [8]–[14]. This method has provided high accuracy in many cases; however, temporal iteration techniques that provide good accuracy for large-scale models typically require small time steps, significant additional computations, or storage of wavefields from additional time steps [13], so that the efficiency advantages of the pseudospectral approach are less than might first be expected. The k -space family of methods [1]–[7] can overcome this problem by providing explicit temporal propagators related to the Green's function for wave propagation in k - t (spatial frequency and time) space.

The present paper presents a simplified derivation of the k -space method using a differential representation of the wave propagation equations. The spatial part of the wave propagation equations is solved by Fourier transformation in a manner analogous to past pseudospectral methods; this derivation is shown to be theoretically equivalent to previous integral formulations of the k -space method. Temporal iteration is performed using a k - t space propagator [2], which is shown to be exact for homogeneous media and, in general, provides much greater accuracy and stability than leapfrog iteration (in which temporal derivatives are evaluated using second-order accurate finite differences) without significant additional computation or storage requirements. Thus, the k -space method provides spatial and temporal accuracy ideal for large-scale models of acoustic propagation in weak scattering media.

Subsequently, a derivation of the k -space method is presented for propagation in fluid media with spatially dependent sound speed and density. For several canonical forward problems relevant to ultrasonic imaging, the

accuracy and efficiency of the k -space method is compared with a pseudospectral method employing leapfrog iteration and also with a 2-4 finite difference time-domain method. The k -space and finite difference methods are also used in an example computation for a large-scale, two-dimensional tissue model. Another example computation illustrates the efficiency of the k -space method for three-dimensional scattering computations. Possible extensions of the present k -space method, including multiple relaxation effects for absorption, absorbing boundary conditions, inclusion of elastic and nonlinear acoustic effects, and parallelization, are discussed.

II. THEORY

A. Derivation of the k -Space Method

The k -space method for solving the acoustic scattering problem is briefly derived subsequently. The derivation is simpler than those previously published and also provides some new insight regarding the remarkable accuracy and stability characteristics of the k -space method.

The method is applicable to large-scale modeling of linear ultrasonic propagation in soft tissues, which are modeled here as fluid media with spatially dependent sound speed and density. Although the k -space method described subsequently can be extended to include absorption effects, acoustic nonlinearity, and shear-wave propagation, these effects are neglected in this derivation for simplicity.

For a fluid medium with spatially dependent sound speed and density, the linear acoustic wave equation is [15]

$$\nabla \cdot \left(\frac{1}{\rho(\mathbf{x})} \nabla p(\mathbf{x}, t) \right) - \frac{1}{\rho(\mathbf{x}) c(\mathbf{x})^2} \frac{\partial^2 p(\mathbf{x}, t)}{\partial t^2} = 0 \quad (1)$$

where $p(\mathbf{x}, t)$ is the acoustic perturbation in pressure, $\rho(\mathbf{x})$ is the spatially dependent density, and $c(\mathbf{x})$ is the spatially dependent sound speed.

By defining the normalized wavefield $f(\mathbf{x}, t) \equiv p(\mathbf{x}, t) / \sqrt{\rho(\mathbf{x})}$, as performed in a number of previous studies (e.g., [16], [17]), the first-order derivative term can be eliminated from (1). Details of this step are given in [6]. When the wavefield is also split into incident and scattered parts, such that $f(\mathbf{x}, t) = f_i(\mathbf{x}, t) + f_s(\mathbf{x}, t)$, a wave equation for the scattered field can be written

$$\nabla^2 f_s(\mathbf{x}, t) - \frac{1}{c_0^2} \frac{\partial^2 f_s(\mathbf{x}, t)}{\partial t^2} = \frac{1}{c_0^2} \left(q(\mathbf{x}, t) + \frac{\partial^2 v(\mathbf{x}, t)}{\partial t^2} \right). \quad (2)$$

The terms on the right-hand side are effective sources associated with density and sound speed variations, which are defined as

$$q(\mathbf{x}, t) = c_0^2 \sqrt{\rho(\mathbf{x})} \nabla^2 \left(1 / \sqrt{\rho(\mathbf{x})} \right) f(\mathbf{x}, t) \quad (3)$$

and

$$v(\mathbf{x}, t) = \left(\frac{c_0^2}{c(\mathbf{x})^2} - 1 \right) f(\mathbf{x}, t). \quad (4)$$

The incident wavefield $f_i(\mathbf{x}, t)$ is required to satisfy the usual wave equation without any source terms [i.e., the D'Alembertian operator from the left-hand side of (2), applied to $f_i(\mathbf{x}, t)$, is equal to zero]. Thus, the total wavefield $f(\mathbf{x}, t)$ also satisfies (2) identically, so that the numerical algorithm developed for the scattered field is equally applicable to the total field.

With the additional definition of an auxiliary field $w(\mathbf{x}, t) = f_s(\mathbf{x}, t) + v(\mathbf{x}, t)$, (2) can be rewritten in k -space as the coupled set of equations

$$\frac{\partial^2 W(\mathbf{k}, t)}{\partial t^2} = (c_0 k)^2 [V(\mathbf{k}, t) - W(\mathbf{k}, t)] - Q(\mathbf{k}, t), \quad (5)$$

$$V(\mathbf{k}, t) = \mathbf{F} \left[\left(1 - \frac{c(\mathbf{x})^2}{c_0^2} \right) [f_i(\mathbf{x}, t) + w(\mathbf{x}, t)] \right], \quad (6)$$

$$Q(\mathbf{k}, t) = c_0^2 \mathbf{F} \left[\sqrt{\rho(\mathbf{x})} \nabla^2 \left(\sqrt{\frac{1}{\rho(\mathbf{x})}} [f_i(\mathbf{x}, t) + w(\mathbf{x}, t) - v(\mathbf{x}, t)] \right) \right] \quad (7)$$

where \mathbf{F} denotes spatial Fourier transformation, and capital letters indicate spatially Fourier transformed quantities.

For each point in k -space, (5) represents an independent ordinary differential equation equivalent to the standard simple harmonic oscillator equation with the source terms $(c_0 k)^2 V$ and $-Q$. This ordinary differential equation can be discretized in several ways. For instance, a second-order accurate finite difference representation of the second-order time derivative allows (5) to be written as

$$W(\mathbf{k}, t + \Delta t) - 2W(\mathbf{k}, t) + W(\mathbf{k}, t - \Delta t) \approx (c_0 k \Delta t)^2 \left[V(\mathbf{k}, t) - W(\mathbf{k}, t) - \frac{Q(\mathbf{k}, t)}{(c_0 k)^2} \right] \quad (8)$$

where Δt is the time step. This is known as leapfrog iteration; use of (8) in the current method is analogous to commonly used pseudospectral approaches [13], [14]. (Although increased accuracy can be achieved by higher order methods such as fourth-order Adams-Bashforth or Adams-Moulton iteration, these methods have the disadvantage of requiring storage of the entire computational grid for additional time steps [12], [13].)

A more accurate form of the temporal iterator is obtained using a nonstandard finite difference approach. For the homogeneous simple harmonic oscillator equation, an exact discretization is known [18]. (That is, for any temporal and spatial step sizes, the discrete difference equations yield exactly the same solutions as the continuous differential equations. A similar exact discretization for the linear

part of the Korteweg-de Vries equation was presented in [19].) Use of this nonstandard discretization leads to the following discrete form of (5):

$$W(\mathbf{k}, t + \Delta t) - 2W(\mathbf{k}, t) + W(\mathbf{k}, t - \Delta t) = 4 \sin^2 \left(\frac{c_0 k \Delta t}{2} \right) \left[V(\mathbf{k}, t) - W(\mathbf{k}, t) - \frac{Q(\mathbf{k}, t)}{(c_0 k)^2} \right]. \quad (9)$$

Because the discretization employed is exact for the simple harmonic oscillator equation, (9) is exactly equivalent to the differential equation, (5), for the case of a homogeneous medium [i.e., $V(\mathbf{k}, t) = Q(\mathbf{k}, t) = 0$]. Numerical results shown subsequently indicate that high accuracy is also achieved for weak scattering media, in which case $V(\mathbf{k}, t) \ll W(\mathbf{k}, t)$ and $Q(\mathbf{k}, t) \ll W(\mathbf{k}, t)$. The present discretization method is equivalent to that employed by Bojarski (the form given in [2] follows after some trigonometric manipulation); however, previous derivations of this method have been based on approximations to an integral representation of (5) [2], [6]. It may also be noted that (8) and (9) are equivalent in the limit of small Δt . However, results shown subsequently indicate that, for weak scattering media, use of the k - t propagator (9) provides much greater accuracy for larger time steps.

In numerical implementation of the k -space algorithm, (5) is used to advance the auxiliary field $W(\mathbf{k}, t)$ in time. Eq. (6) and (7) represent updates of the effective scattering sources v and q and their spatial Fourier transformation to yield the k -space effective sources V and Q . Notable is that the effective source v is directly proportional to the square of the sound speed variation of the medium, and the effective source q is directly proportional to the Laplacian of $1/\sqrt{\rho(\mathbf{x})}$. Thus, for a piecewise constant inhomogeneous medium, v may be non-zero everywhere, but q is nonzero (and singular) only on borders between regions.

The present k -space algorithm can now be summarized as follows:

- Step 1: set any initial conditions for $w(\mathbf{x}, t)$ and spatially Fourier transform [by fast Fourier transform (FFT)] to obtain initial conditions for $W(\mathbf{k}, t)$
- Step 2: define the incident wave $f_i(\mathbf{x}, t)$ on the entire grid ($f_i(\mathbf{x}, t)$ can be identically zero)
- Step 3: compute $v(\mathbf{x}, t)$ and transform to obtain $V(\mathbf{k}, t)$ (6)
- Step 4: compute $q(\mathbf{x}, t)$ and transform to obtain $Q(\mathbf{k}, t)$ (7)
- Step 5: evaluate $W(\mathbf{k}, t + \Delta t)$ (9) and inverse transform to obtain $w(\mathbf{x}, t + \Delta t)$
- Step 6: set $t \rightarrow t + \Delta t$ and go to step 2

This method requires three fast Fourier transform operations per time step (one each for steps 3, 4, and 5 of the algorithm enumerated above).

Also notable is that the algorithm is directly applicable to one-dimensional, two-dimensional, and three-dimensional propagation. This is possible because the k - t space Green's function has an identical form for any number of spatial dimensions [2]. For example, to implement

the present methods for two-dimensional computations, the algorithm just outlined is simply employed using two-dimensional Fourier transforms. The three-dimensional version of the algorithm is formally identical but with three-dimensional Fourier transforms.

To distinguish between the standard leapfrog iteration method and the improved method used here, the following nomenclature is used in the present paper. The algorithm employing (9) is referred to as a k -space method, and the corresponding algorithm employing (8) for temporal iteration is referred to as a leapfrog pseudospectral method. This nomenclature is used because the algorithm employing (9) is mathematically equivalent to an extended form of Bojarski's k -space method [2] cast in terms of differential equations rather than integral equations. The algorithm employing (8) is referred to as pseudospectral because it is mathematically equivalent to a conventional "method of lines" pseudospectral algorithm with leapfrog iteration [12]. [A conventional pseudospectral algorithm of this form would employ the spatial inverse Fourier transform of (8) for temporal iteration.]

B. Temporal and Spatial Sampling Criteria

To determine the usable range of spatial and temporal sampling rates for the present k -space method, limits on the stability and accuracy of the method can be evaluated analytically.

The stability of the k -space and leapfrog pseudospectral methods derived previously can be evaluated using standard, linear von Neumann stability analysis [20]. Using this technique, the difference equations that comprise (8) and (9) are applied to a test function

$$W_{\text{test}}(\mathbf{k}, n\Delta t) = \vartheta(\mathbf{k})^n \psi(\mathbf{k}) \quad (10)$$

where $\psi(\mathbf{k})$ is a spatial-frequency domain eigenmode and $\vartheta(\mathbf{k})$ is a temporal amplification factor. If a difference equation admits solutions with $|\vartheta(\mathbf{k})| > 1$ for any vector wavenumber \mathbf{k} , errors may grow exponentially with time, and the solution is thus unstable. If $|\vartheta(\mathbf{k})| \leq 1$ for all wavenumbers, then the solution is numerically stable. For simplicity, the present stability computation is performed in the absence of density variations; the incident wave $f_i(\mathbf{x}, t)$ is assumed (without loss of generality) to be zero. To obtain limiting stability criteria, the worst case sound speed inhomogeneity $c(\mathbf{x}) = c_{\text{max}}$ is also assumed.

Application of this technique to (8), which represents a leapfrog pseudospectral approach, yields a quadratic equation for $\vartheta(\mathbf{k})$. The resulting stability condition is

$$c_{\text{max}} k_{\text{max}} \Delta t \leq 2 \quad (11)$$

where c_{max} is the maximum sound speed in the region of computation; $k_{\text{max}} = \pi/\Delta x$ is the maximum wavenumber in the discrete Fourier transforms used to compute $W(\mathbf{k}, \mathbf{t})$; and Δt and Δx , respectively, are the temporal and spatial steps employed. Using the standard definition

for a Courant-Friedrichs-Lewy (CFL) number [21], the stability condition

$$\text{CFL} \equiv \frac{c_0 \Delta t}{\Delta x} \leq \frac{2}{\pi} \frac{c_0}{c_{\text{max}}} \quad (12)$$

is obtained for the leapfrog pseudospectral method represented by (8).

Application of the same analysis to the k -space iterator of (9) yields the stability condition

$$\sin \frac{\pi \text{CFL}}{2} \leq \frac{c_0}{c_{\text{max}}}. \quad (13)$$

This condition has the remarkable result that, for media with $c(\mathbf{x}) \leq c_0$ everywhere, the linear numerical stability of the k -space method is unconditional. However, for any medium, an upper limit on the time step still arises from the requirement of sampling at the Nyquist rate: that is, the time step should be sufficiently small to allow two samples per period for the highest frequency component of the computed field. Thus, the temporal sampling criterion can be written

$$\Delta t \leq \frac{1}{2f_{\text{max}}} = \frac{\pi}{c_{\text{max}} k_{\text{max}}} = \frac{\Delta x}{c_{\text{max}}} \quad (14)$$

or simply $\text{CFL} \leq c_0/c_{\text{max}}$. The stability criterion (13) is met whenever the Nyquist sampling criterion (14) is met; thus, the Nyquist sampling criterion is more restrictive.

For the spatial discretization, a Nyquist criterion based on the maximum spatial frequency $k_{\text{max}} = \pi/\Delta x$ is met for any step size Δx . However, the inhomogeneous medium will be inaccurately represented (aliased) if its Fourier transform has significant spatial-frequency components beyond k_{max} . Aliasing is a particular problem when the medium contains discontinuities, which correspond to infinite spatial frequency content; removal of errors associated with discontinuities is discussed in the following section.

C. Effects of Discontinuities

The Fourier transforms performed in the present k -space algorithm can lead to numerical artifacts (related to the Gibbs phenomenon) when the inhomogeneous medium contains discontinuities in sound speed or density. To avoid such artifacts, the scattering object can be spatially filtered to smooth any discontinuities. That is, the spatially dependent sound speed $c(\mathbf{x})$ and density $\rho(\mathbf{x})$ can be replaced by filtered functions of the form

$$u_{\text{filtered}}(\mathbf{x}) = \mathbf{F}^{-1}[U(\mathbf{k}) \phi(\mathbf{k})] \quad (15)$$

in which the Fourier transform $U(\mathbf{k})$ of the function $u(\mathbf{x})$ is multiplied by a low-pass spatial frequency filter $\phi(\mathbf{k})$. The function $U(\mathbf{k})$ should be represented as accurately as possible; for example, exact Fourier transforms of simply shaped inhomogeneities can be used when available. Subsequently, the exact Fourier transform of a two-dimensional disk is employed for filtered representations of an infinite cylinder.

In the present study, the filter employed is the half-band filter [22]

$$\phi_H(k) = \begin{cases} 1, & k/k_{\max} < 1/2 \\ f(k/k_{\max} - 1/2), & 1/2 \leq k/k_{\max} \leq 3/2 \end{cases} \quad (16)$$

where

$$f(\theta) = \frac{1}{2} + \frac{9}{16} \cos(\pi\theta) - \frac{1}{16} \cos(3\pi\theta) \quad (17)$$

and k is the magnitude of the spatial frequency vector \mathbf{k} .

This filter defines a smoothly tapered window that causes no attenuation of spatial frequencies below $k_{\max}/2$ and drops to one-half amplitude (−6 dB) at the spatial frequency k_{\max} . Zero amplitude is reached at the spatial frequency $3/2 k_{\max}$, which exceeds the spatial frequency range of the discrete Fourier transforms employed in the k -space algorithm, so that aliasing error is not eliminated by the half-band filter. However, a strict bandlimiting filter was found to cause excessive loss of high spatial frequency components in the medium, so that scattering amplitude near the backscatter direction was greatly reduced. The half-band filter of (16) was found to greatly reduce Gibbs phenomenon artifacts and maintain enough high spatial frequency components of inhomogeneities to provide accurate backscatter results.

For inhomogeneous media, exact Fourier transforms are not generally available. However, artifacts associated with discontinuities can still be removed by the methods given previously. For example, a finely sampled representation of the medium could be filtered using (15) and then decimated to the desired spatial step size.

III. NUMERICAL METHODS

Numerical implementation of the k -space algorithm was accomplished using the algorithm described previously. The normalized incident wave $f_i(\mathbf{x}, t)$ was defined as a plane wave with Gaussian temporal shape:

$$f_i(\mathbf{x}, t) = \rho(\mathbf{x})^{-\frac{1}{2}} \sin(\omega_0\tau) e^{-\tau^2/(2\sigma^2)} \quad (18)$$

where τ is the retarded time $\tau = t - (x - x_0)/c_0$ and x_0 is the initial central position of the wavefield. This incident wave was implicitly specified using initial conditions (as for the incident plane wave in [23]) rather than explicitly updated at each time step. Boundary conditions were implicitly periodic at each edge of the computational domain because of the inherent periodicity of the fast Fourier transforms employed.

Wavefields were computed on two-dimensional grids that were large enough to avoid influence of “wraparound” error within the temporal window of interest. All k -space computations were performed on square grids of size N by N . Prior to execution of the main computation loop, the Laplacian occurring in (7) was evaluated using second-order accurate, centered finite difference representations of

the second derivative in each direction. Within the main computational loop, all spatial derivatives were evaluated by Fourier transformation, implemented using an FFT algorithm [24]. For maximum FFT efficiency, grid sizes N were chosen to be integers with prime factors no greater than three.

To reduce any spatial anisotropy associated with the rectangular grid shape, the spatial frequency time-domain wavefield $W(\mathbf{k}, t + \Delta t)$ was windowed using the radially symmetric window

$$\phi(\mathbf{k}) = H(k_{\max} - k) \quad (19)$$

before inversion to yield $w(\mathbf{x}, t + \Delta t)$ (i.e., within step 5 in the algorithm enumerated previously). In (19), H is, as before, the Heaviside step function, k_{\max} is the maximum wavenumber magnitude (equal to $\pi/\Delta x$ because the spatial frequency range sampled extends from $-\pi/\Delta x$ to $\pi/\Delta x$ in each direction), and k is the magnitude of the vector wavenumber \mathbf{k} . In some cases, the medium properties $c(\mathbf{x})$ and $\rho(\mathbf{x})$ were also smoothed by windowing in the spatial-frequency domain using (16) with a wavenumber cutoff of $k_{\max} = \pi/\Delta x$.

For comparison, wavefields were also computed using a second-order in time, fourth-order in space finite difference method, described in [21], [23], [25]–[27]. As for the k -space computations, the incident wave was specified by a single initial condition rather than updated at each time step. Periodic boundary conditions were applied on all sides of the grid. Time steps were determined using a CFL number of 0.25, which is a natural choice for this finite difference method [26]. As in [23] and [28], computations were performed at each time step only on portions of the grid where the wavefields were nonzero; this reduces the required computation time for the finite difference method by about one-half.

To test the k -space and finite difference methods quantitatively, benchmark computations were performed using an exact series solution for the scattering of a plane wave by a fluid cylinder [29]. The sampling rate and waveform shape were chosen to match the time-domain simulation data for the case of interest. The pressure field was then computed for each frequency component with relative magnitude within 60 dB of the peak magnitude. Each single frequency computation truncated the series at the term with a relative contribution less than 10^{-12} times the sum of all terms. The frequency-domain scattered fields were then inverted by FFT to obtain numerically exact solutions for the time-domain pressure fields at the simulated measurement points. An exact time-domain solution for scattering from a fluid sphere was also obtained using an analogous approach.

Benchmark studies of accuracy were performed using a cylinder with radius 2.0 mm and acoustic properties of human fat and a background medium with acoustic properties of water at body temperature. Rationale for use of these values is discussed in [23]. The cylinder had a sound speed of 1.478 mm/ μ s and a density of 0.950 g/cm³; the background medium had a sound speed of 1.524 mm/ μ s

$$\begin{aligned}
p_{\text{interp}}(x, y) &= \sum_{x_i} \sum_{y_i} \frac{\sin(\pi(x - x_i)/\Delta x)}{\pi(x - x_i)/\Delta x} \frac{I_0[\beta(1 - [(x - x_i)/(m\Delta x)]^2)^{1/2}]}{I_0[\beta]} \\
&\times \frac{\sin(\pi(y - y_i)/\Delta x)}{\pi(y - y_i)/\Delta x} \frac{I_0[\beta(1 - [(y - y_i)/(m\Delta x)]^2)^{1/2}]}{I_0[\beta]} \times p(x_i, y_i), \\
x - m\Delta x &\leq x_i < x + m\Delta x, \\
y - m\Delta x &\leq y_i < y + m\Delta x
\end{aligned} \tag{20}$$

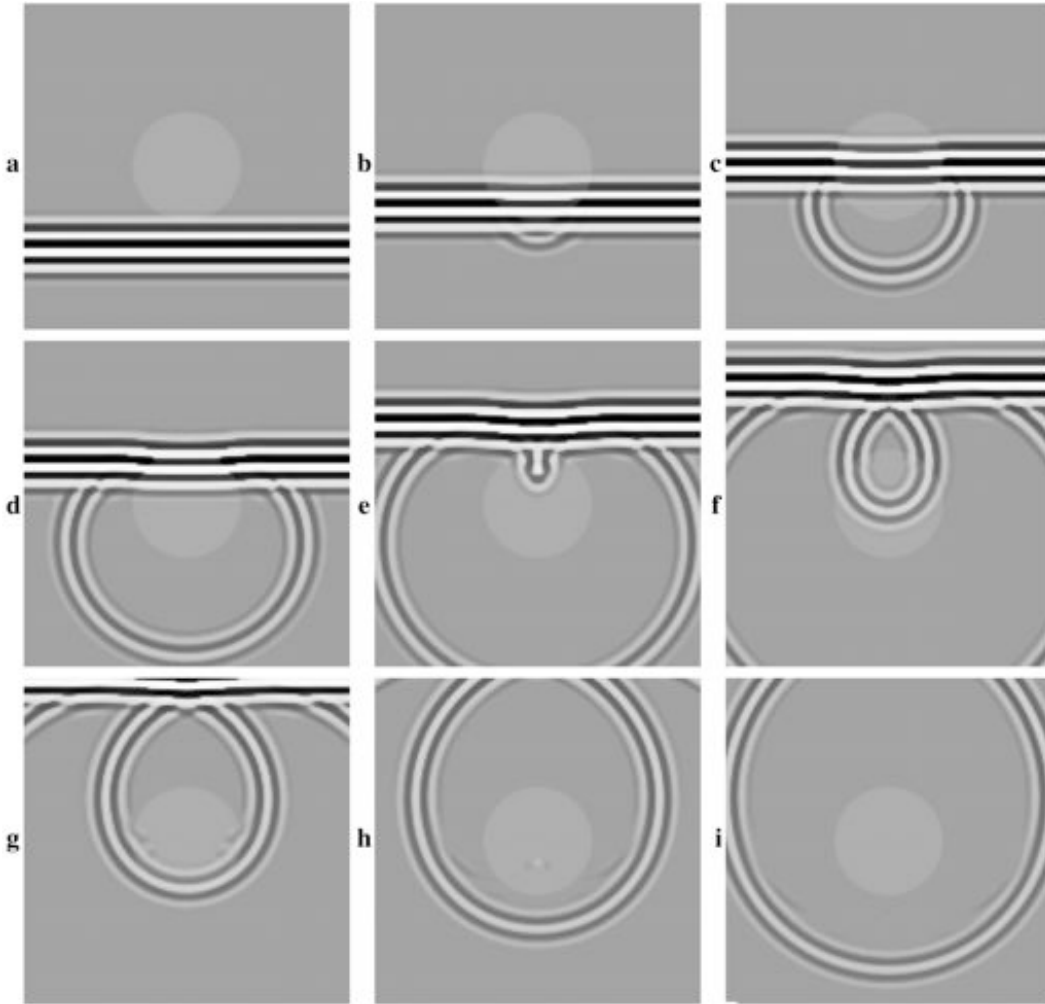


Fig. 1. Time history of total acoustic pressure computed by the k -space method for a cylinder with a 2.0-mm radius and fat-mimicking acoustic properties. The cylinder is sketched as a light gray region. The first panel shows the wavefield impinging on the cylinder at time $t = 0.98 \mu\text{s}$, and subsequent panels (progressing from left to right and top to bottom) show the total wavefield at intervals of $0.98 \mu\text{s}$. The acoustic pressure is plotted in all panels using a bipolar logarithmic scale with a 60 dB dynamic range.

and a density of 0.993 g/cm^3 . The scattering geometry is as shown in Fig. 1. The incident pulse was a plane wave with Gaussian temporal characteristics, a temporal Gaussian parameter $\sigma = 0.25 \mu\text{s}$, and a central starting position of $x = -4.5 \text{ mm}$ at time zero. For this pulse, a nominal maximum frequency is 4.43 MHz, corresponding to the spectral point 40 dB down from the center frequency (for the benchmark problem, this frequency corresponds to a

minimum wavelength of 0.33 mm). The k -space, leapfrog pseudospectral, finite difference, and exact methods described previously were used to compute time histories of the total pressure field at 128 equally spaced “measurement” points spanning a circle of radius 2.5 mm concentric to the cylinder. The pressure was interpolated using a two-dimensional low-pass interpolation filter implemented by the formula [30] [(20), see above], where I_0 is the zero-

order modified Bessel function of the first kind, and β is the Kaiser window coefficient, taken here to be 7.0. This choice of β provides a filter with flat response up to about $0.6 k_{\max}$ and sidelobes at the -70 dB level.

The domain size for each k -space, pseudospectral, and finite difference computation employing this cylinder was 18×18 mm².

Further studies of accuracy were performed using a cylinder of radius 10 mm. Other parameters were as described previously for the small problem, except that the radius of the measurement circle was 12.5 mm and the starting position of the wavefront was $x = -14.5$ mm. The k -space method was employed to compute two cases corresponding to unsmoothed and smoothed contrast functions, using a spatial step of four points per minimum wavelength and a CFL number of 0.5. In each k -space computation for this cylinder, the domain size employed was 72×72 mm². The finite difference method was employed to compute a single case using a spatial step of 14 points per minimum wavelength, a CFL number of 0.25, and a domain size of 72×60 mm.

To evaluate the relative accuracy and efficiency of the k -space and finite difference methods for a high contrast scatterer, computations were also performed using a cylinder of radius 2.0 mm with the sound speed and density of human bone. The values employed were a sound speed of 3.54 mm/ μ s and a density of 1.99 g/cm³ as in [28]. The incident pulse, receiver, and computational domain characteristics were identical to those for the 2.0 mm “fat” cylinder case described previously.

In all of the previously mentioned accuracy tests, a quantitative measure of the accuracy was obtained using the time-domain L^2 error of each numerically computed pressure field $p_{\text{num}}(\mathbf{x}, t)$ versus the corresponding exact series solution $p_{\text{exact}}(\mathbf{x}, t)$. This quantity has the definition

$$\epsilon = \frac{\|p_{\text{num}}(\mathbf{x}_r, t) - p_{\text{exact}}(\mathbf{x}_r, t)\|}{\|p_{\text{exact}}(\mathbf{x}_r, t)\|} \quad (21)$$

where $\|p(\mathbf{x}_r, t)\|$ is the L^2 norm [31] of a matrix composed of the time-domain signal $p(\mathbf{x}, t)$ for all receiver points \mathbf{x}_r and all time samples computed. Eq. (21) represents an accuracy criterion that is much stricter than more general criteria, such as comparison of the rms waveform amplitude or the amplitude and phase at the center frequency. To achieve a low L^2 error by the definition of (21), both the waveform amplitude and phase must be accurately computed for all significant frequency components of the field.

The use of the present k -space method in a more realistic two-dimensional simulation of ultrasonic propagation was also tested. For this purpose, a cross-sectional tissue map of the human chest wall [28] was used as the simulated medium. A pulse center frequency of 3.0 MHz was employed together with a temporal Gaussian parameter of 0.3127 μ s; these parameters correspond to the highest center frequency employed in the simulation study reported in [28]. The corresponding nominal minimum wavelength is 0.34 mm. The k -space computation employed four points

per minimum wavelength, a CFL number of 0.5, and a grid size of 54.9×54.9 mm². The finite difference computation employed 14 points per minimum wavelength, a CFL number of 0.25, and a grid size of 38.5×29.7 mm². As in [23] and [28], periodic boundary conditions were applied on the sides perpendicular to the wavefront; first-order radiation boundary conditions [23] were applied on the sides parallel to the wavefront.

Finally, to illustrate the efficiency and accuracy of the present k -space method for three-dimensional computations, scattering from a penetrable sphere with acoustic properties of human muscle (speed, 1.547 mm/ μ s; density, 1.090 g/cm³ [23]) was computed. The sphere radius was 1.5 mm; time-domain pressure waveforms were recorded at 128 equally spaced measurement points on the sphere surface (in the $\phi = 0$ plane). The computation employed an incident pulse identical to that for the cylinder simulations described previously, a spatial step of four points per minimum wavelength and a CFL number of 0.5. The total pressure wavefield was computed for a time duration of 7.3 μ s on a three-dimensional grid of dimensions $10.66 \times 10.66 \times 10.66$ mm³. The accuracy of this computation was assessed by evaluating the L^2 error between the k -space and exact solutions using (21).

IV. NUMERICAL RESULTS

An example k -space computation, performed using the 2.0-mm cylinder with acoustic properties of human fat, is illustrated in Fig. 1. The cylinder is also sketched in each panel. For the computation shown, smoothed sound speed and density functions were obtained by filtering the analytic spatial Fourier transform of the cylinder using (16). The time history of the total wavefield is shown as computed by the k -space method for a spatial step size of four points per minimum wavelength and a CFL number of 0.5. Details visible include a scattered wave from the edge nearest the initial wavefront (c), weak focusing near the trailing edge of the cylinder (e), scattering from the trailing edge [(f)–(i)], and low level multiple scattering [(g)–(h)].

Results of accuracy benchmarks for the k -space and leapfrog pseudospectral methods described previously are shown in Fig. 2. Each of these computations was made using the 2.0-mm cylinder described previously and a spatial step size of four points per maximum wavelength. The results show that the k -space method employing the k - t space propagator of (9) provides much higher accuracy than the pseudospectral method employing the leapfrog propagator of (8). The two methods provide equivalent results for very small time steps (CFL numbers less than about 0.1), but the k -space method maintains its highest accuracy up to a CFL number of about 0.4. In contrast, the pseudospectral method rapidly increases in error for CFL numbers above 0.1.

Error results for the pseudospectral computations shown in Fig. 2 are not given for CFL numbers above 0.6 because the computation was unstable for higher CFL numbers i.e., computed fields incurred spurious exponen-

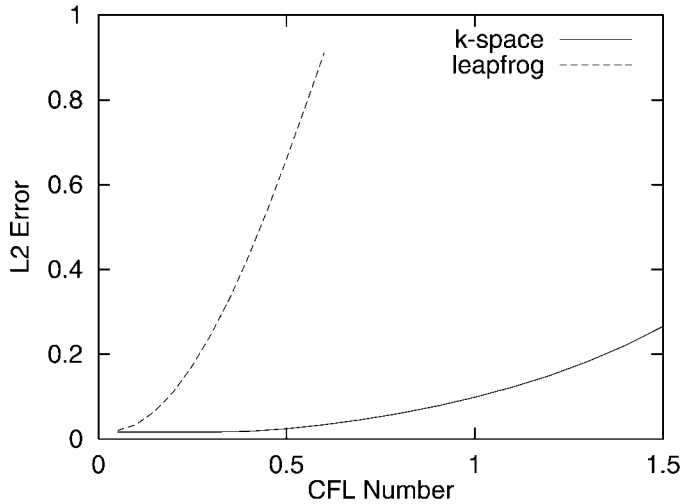


Fig. 2. Time-domain comparison of accuracy for the k -space and leapfrog pseudospectral methods as a function of Courant-Friedrichs-Lewy (CFL) number. Each test used the “fat” cylinder (2.0-mm radius) and a spatial step size of four points per minimum wavelength.

tial growth, resulting in numerical overflow. This observation of instability is consistent with the linear stability limit of 0.6366 given by (12) for this case. The k -space method did not incur any numerical instability for the range of CFL numbers investigated, so that the method is observed to be unconditionally stable as predicted for $c(\mathbf{x}) \leq c_0$. However, the error of this method grows as the CFL number approaches and exceeds unity, consistent with the Nyquist sampling criterion given by (14).

Pseudospectral methods employing higher order time integration achieve higher accuracy than the leapfrog iteration used as a comparison here. However, tests of the present k -space method and a pseudospectral method employing fourth-order Adams-Bashforth time integration have shown trends similar to that seen in Fig. 2 [32]. Specifically, for weak scattering media, the k -space method yields similar accuracy for time steps two to three times larger than those required by the higher order pseudospectral method described in [13].

The relative accuracy of the k -space method and the 2-4 finite difference method are compared in Fig. 3 as a function of the spatial step size. For these computations, the CFL number of the k -space computations was held constant at 0.5, consistent with the CFL-accuracy relationship shown in Fig. 2; the CFL number of the finite difference computations was held at 0.25 [26]. Both methods achieve high accuracy for finer grid spacings; however, the k -space method achieves higher accuracy for much larger spatial step sizes. The L^2 error drops below 0.05 for k -space computations, employing only three points per minimum wavelength; achievement of the same accuracy criterion requires 14 points per minimum wavelength for the finite difference computations. This difference suggests that storage requirements for k -space computations can be much smaller than those for finite difference computations of comparable accuracy, on the order of 12 times smaller

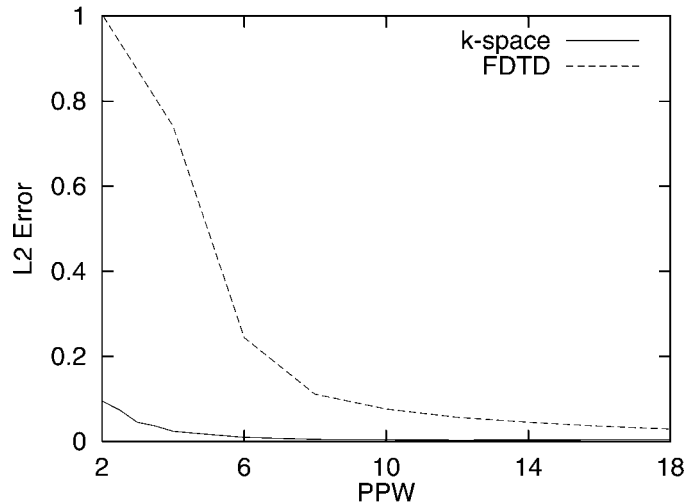


Fig. 3. Time-domain comparison of accuracy for the k -space and 2-4 finite difference time-domain methods as a function of the spatial step size in points per minimum wavelength (PPW). Each test used the “fat” cylinder (2.0-mm radius). Courant-Friedrichs-Lewy (CFL) numbers were 0.5 for the k -space method and 0.25 for the finite difference time-domain method.

for two-dimensional computations and 43 times smaller for three-dimensional computations.

Visual comparison of simulated waveforms for the 2.0-mm cylinder is shown in Fig. 4. Waveforms in this figure are those computed using the k -space (four points per minimum wavelength; CFL number, 0.5; both unsmoothed and smoothed contrast functions), finite difference time-domain (14 points per minimum wavelength; CFL number, 0.25), and exact methods. The k -space solution for the unsmoothed cylinder shows a small time-domain L^2 error (0.0243) but also exhibits spurious waves (nearly 60 dB down from the peak pressure amplitude) between the two main arrivals. These spurious waves are removed by use of the k -space method with smoothed medium parameters [i.e., $\rho(\mathbf{x})$ and $c(\mathbf{x})$ smoothed using (16) with $k_{\max} = \pi/\Delta x$]; the L^2 error is decreased to 0.0214 by this smoothing. The finite difference result bears a strong qualitative resemblance to the exact solution, but the larger L^2 error (0.0454) indicates that phase errors have been introduced by the dispersion inherent to the finite difference method. Computation times [33] were 2.31 min for the k -space method and 1.55 h for the finite difference method, so that the k -space method yields greater accuracy at much less computational cost.

Waveforms for the 10-mm cylinder are shown in Fig. 5 in a format analogous to that of Fig. 4. These results indicate that, as for the smaller cylinder, smoothing of the contrast functions produces a reduction in spurious low amplitude waves. For this problem, unlike the 2.0-mm cylinder discussed previously, this smoothing slightly decreases the overall accuracy. (The time-domain L^2 error is 0.1292 for the smoothed case vs. 0.1288 for the unsmoothed case.) The finite difference solution, using 14 points per wavelength and a CFL number of 0.25, requires much greater storage and computational time and produces waveforms

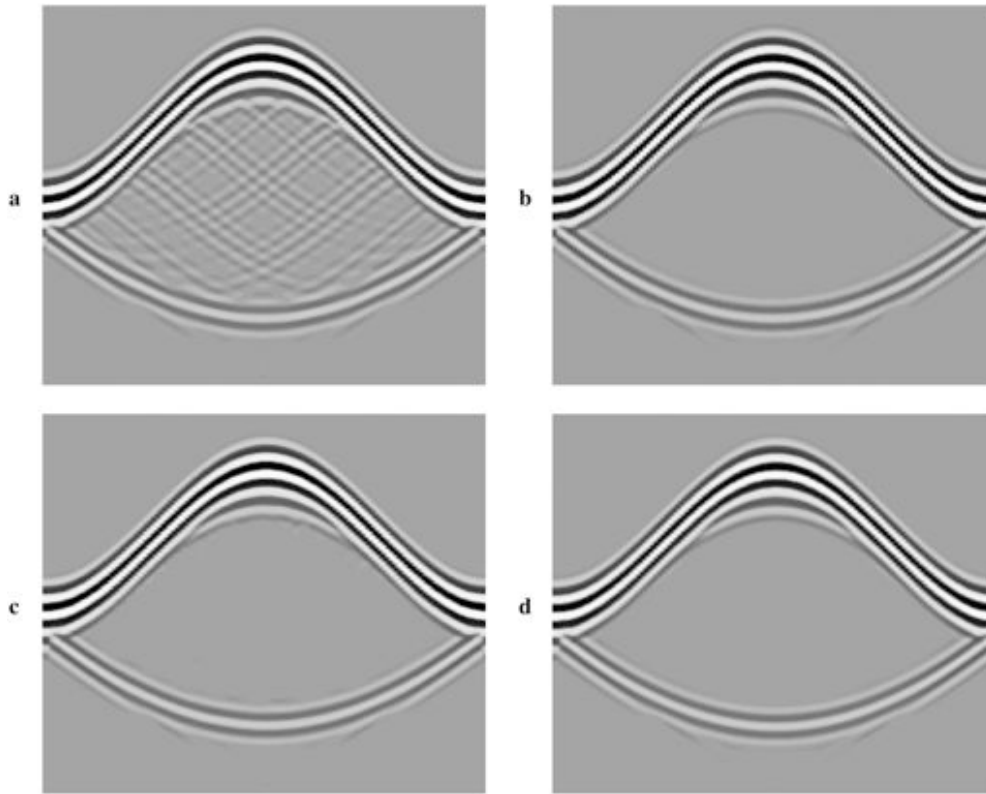


Fig. 4. Computed waveforms for the “fat” cylinder at a radius of 2.5 mm for a cylinder of radius 2.0 mm and a pulse center frequency of 2.5 MHz. The acoustic pressure is shown on a bipolar logarithmic scale with 60 dB dynamic range. The horizontal range of each plot is 360 degrees, covering the entire measurement circle starting with angle 0 (forward propagation). The vertical range of each panel corresponds to a temporal duration of 9 μ s, with $t = 0$ at the top of each plot. a) Unsmoothed object: k -space solution with four points per minimum wavelength, L^2 error = 0.0243; b) smoothed object: k -space solution with four points per minimum wavelength, L^2 error = 0.0214; c) finite-difference solution with 14 points per minimum wavelength, L^2 error = 0.0454; and d) exact solution.

with poorer accuracy (an L^2 error of 0.1794) than the k -space method.

Results for the 2-mm “bone” cylinder are shown in Fig. 6. In this case, the k -space method using a CFL number of 0.5 exhibited numerical instability. This instability is expected because this CFL number exceeds the limit of 0.2833 set by (13). To obtain an appropriate temporal sampling rate, the time step was reduced in proportion to the increase in c_{\max} , resulting in a CFL number of 0.2153. Required computation time for the k -space method was 5.34 min¹; the time-domain L^2 error was 0.3061 for the unsmoothed case and 0.2687 for the smoothed case.

The finite difference method, employing 14 points per wavelength and a CFL number of 0.1076 (also changed in proportion to c_{\max}), achieved an L^2 error of 0.0350 in a computation time of 3.99 h¹. This result indicates that finite difference methods can be much more accurate than k -space methods for scattering problems involving very high contrast inhomogeneities such as bone within soft tissue. However, the k -space solution, as seen in Fig. 6, still shows good qualitative agreement with the exact solution.

The relative inaccuracy of the k -space method for high

contrast scatterers may be associated with aliasing effects, as suggested in [5]. That is, large jumps in spatial contrast functions are associated with significant high frequency components of the corresponding k -space spectra. If the spatial frequency range employed in the k -space algorithm is not sufficiently large, aliasing errors result. Low-pass filtering of the contrast functions would remove this aliasing, but this also introduces additional errors because high spatial frequency components of the scattering medium are lost. The half-band filtering employed here is a compromise that greatly reduces aliasing errors but maintains some contributions from high spatial frequencies (up to the spatial Nyquist rate).

Computational results for a large scale, two-dimensional tissue model are shown in Fig. 7. Waveforms computed by the k -space (four points per minimum wavelength; CFL number, 0.5; no smoothing) and the finite difference models (10 points per minimum wavelength; CFL number, 0.25) were recorded at 130-element apertures composed of simulated point receivers separated by a pitch of 0.21 mm. The results produced by the finite difference method and the k -space method are visually indistinguishable. However, despite the reduced grid size and limited computations employed for the finite difference method, the k -space method was more efficient by about a factor

¹All CPU timings reported in this paper were obtained using a Linux workstation with a 200-MHz AMD K6 processor and 128 MB RAM.

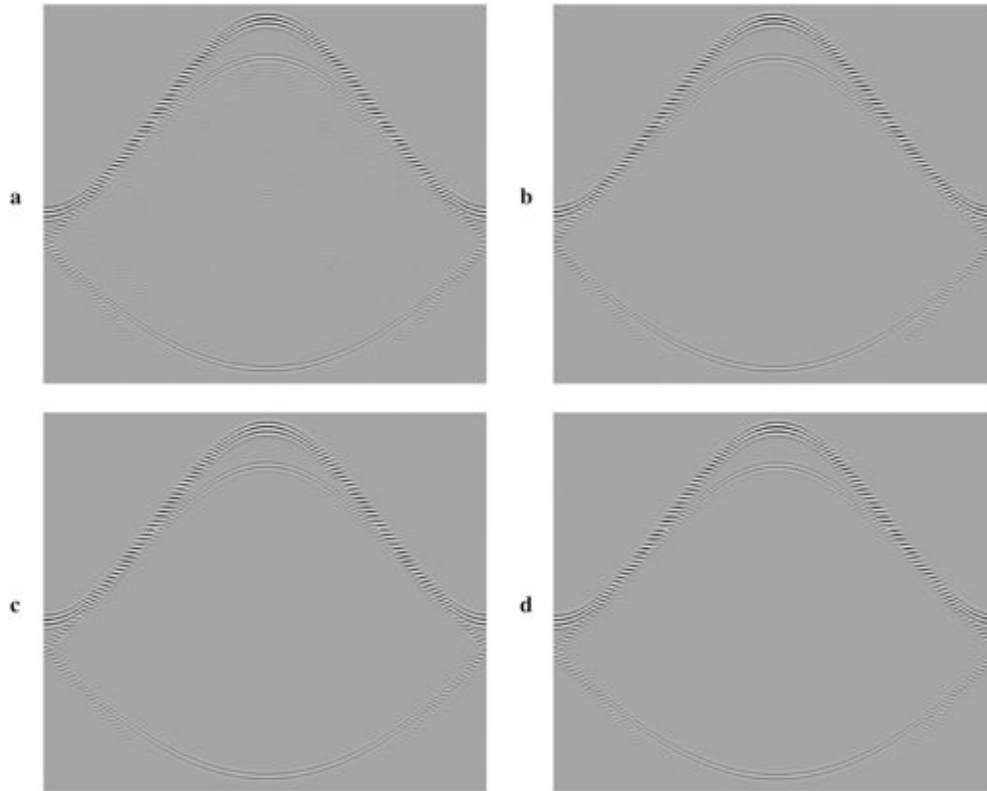


Fig. 5. Computed waveforms at a radius of 12.5 mm for a “fat” cylinder of radius 10.0 mm and a pulse center frequency of 2.5 MHz. The acoustic pressure is shown in each panel using a bipolar logarithmic scale with a 60 dB dynamic range. The horizontal range of each panel is 360 degrees, and the vertical range is 33 μ s. a) Unsmoothed object: k -space solution, L^2 error = 0.1288; b) smoothed object: k -space solution, L^2 error = 0.1292; c) finite-difference solution, L^2 error = 0.1794; and d) exact solution.

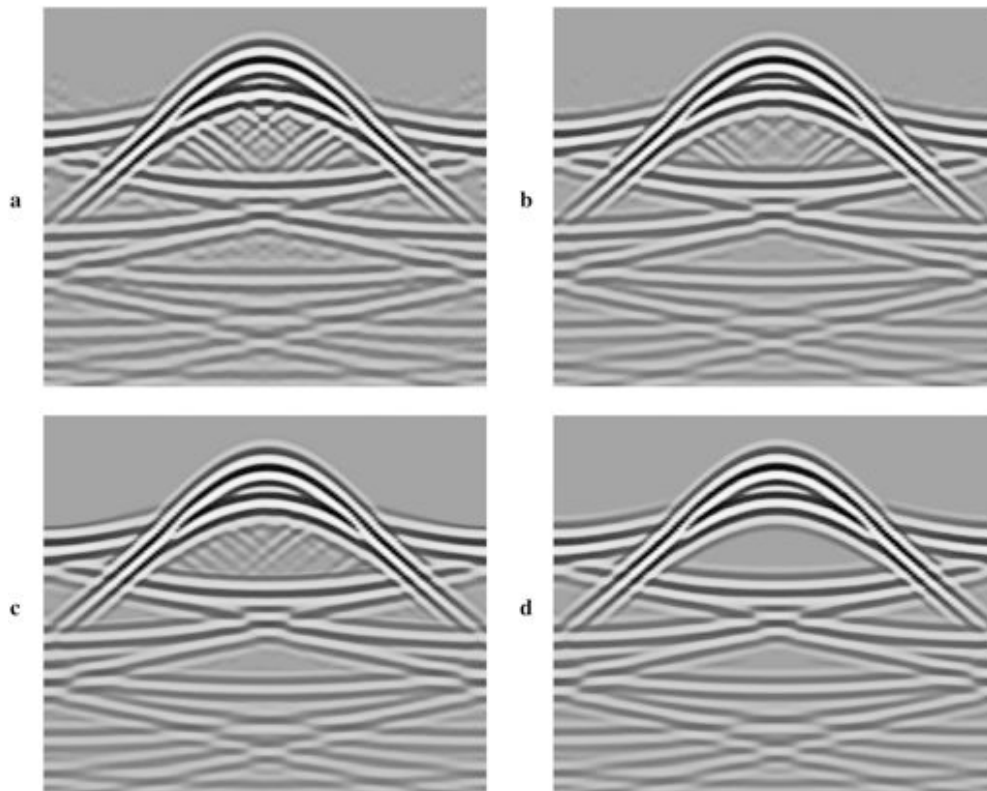


Fig. 6. Computed pressure waveforms at a receiver radius of 2.5 mm for a “bone” cylinder of radius 2.0 mm and a pulse center frequency of 2.5 MHz. The format is the same as in Fig. 4. a) Unsmoothed object: k -space solution, L^2 error = 0.3061; b) smoothed object: k -space solution, L^2 error = 0.2687; c) finite-difference solution, L^2 error = 0.0380; and d) exact solution.

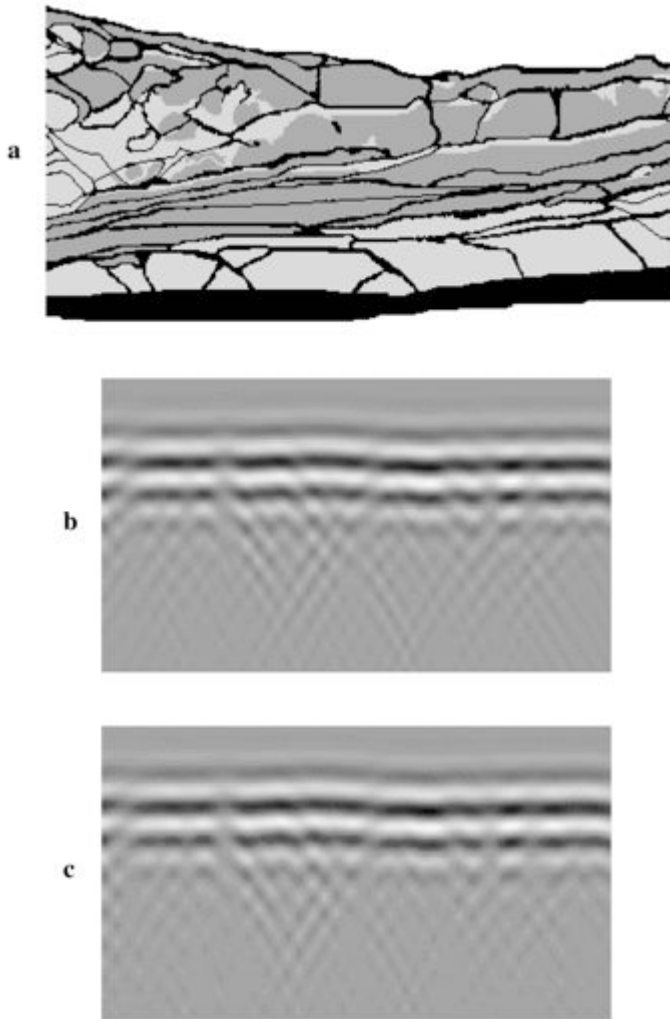


Fig. 7. Comparison of k -space and finite difference methods for a tissue cross-sectional model. a) Chest wall cross section (taken from [24]), with black indicating connective tissue, dark gray indicating muscle, and light gray indicating fat. The region is 33.5 mm wide and 17.2 mm high. b) Transmitted waveforms computed by the k -space method using four points per minimum wavelength and a Courant-Friedrichs-Lewy (CFL) number of 0.5, shown on a bipolar linear gray scale with white indicating maximum positive pressure and black indicating maximum negative pressure. The horizontal range shown is 27.3 mm at the same scale as a. The vertical range is $3.29 \mu\text{s}$. c) Transmitted waveforms computed by the finite difference time-domain method using 10 points per minimum wavelength and a CFL number of 0.25, shown using the same format as b.

of four; the required CPU time for the k -space method was 0.90 CPU h; the corresponding time for the finite difference time-domain method was 4.58 CPU h¹. This discrepancy in efficiency is even more impressive when note is made that the k -space method using four points per minimum wavelength provides significantly higher accuracy than the finite difference method using 14 points per minimum wavelength (as illustrated in Fig. 3). Thus, the present k -space method is suggested to be an appropriate replacement for finite difference methods previously employed to compute propagation through large scale, soft tissue models [23]–[28].

Results of the example three-dimensional computation are shown in Fig. 8. Three-dimensional isosurface renderings of the total pressure wavefield are shown at three instants separated by $0.79 \mu\text{s}$. For the three-dimensional computation, the total computation time required was 1.51 h¹. The L^2 error of the computed waveforms, relative to the exact time-domain solution for scattering from a sphere [29], was 0.0186.

V. EXTENSIONS TO THE k -SPACE METHOD

The present method can be extended in a number of ways to increase its range of applicability in computations of ultrasound tissue interactions.

Absorption effects could be added to the present algorithm in several ways. The most straightforward method for including absorption is to include an ad hoc damping term proportional to $\partial f_s / \partial t$ in (2) [3]–[5]. This approach yields absorption coefficients roughly independent of frequency. Similarly, inclusion of a damping term proportional to $\partial^3 f_s / \partial t^3$ (a thermoviscous approximation) would lead to absorption roughly proportional to the frequency squared [33]. However, neither of these approaches has a rigorous justification for use in models of ultrasound propagation in biological tissue.

A physically justifiable approach for inclusion of absorption in the present algorithm is to consider absorption associated with multiple relaxation processes. The theoretical basis for this approach is presented in [34]; one implementation of this method in a finite difference time-domain algorithm is given in [35]. Because multiple relaxation processes can lead to a variety of frequency-dependent absorption characteristics, this approach provides a possibility of modeling realistic frequency-dependent attenuation in tissue without introduction of nonphysical dispersion or violation of causality. Following the methods presented in [35], absorption caused by multiple relaxation processes can be implemented in a computationally efficient form. Possible alternatives include the time-causal power law absorption formulation of [36].

Another possible extension to the present method is to incorporate the full elastic wave propagation equations. This extension would account for shear wave propagation, which may substantially affect results for propagation models, including bone and other calcified tissue. By applying methods similar to those outlined in [7] to the algorithm described previously, a full elastic k -space method incorporating Fourier space evaluation of spatial derivatives and a k - t space propagator could be derived. Such a method would, as in [7], include separate k - t space propagators for compressional and shear waves.

Boundary conditions of k -space and pseudospectral methods are inherently periodic, so that simple radiation boundary conditions cannot be straightforwardly implemented. One option for absorbing boundary conditions is to include tapered (artificial) absorption functions at each boundary [37]. The technique of perfectly matched layers

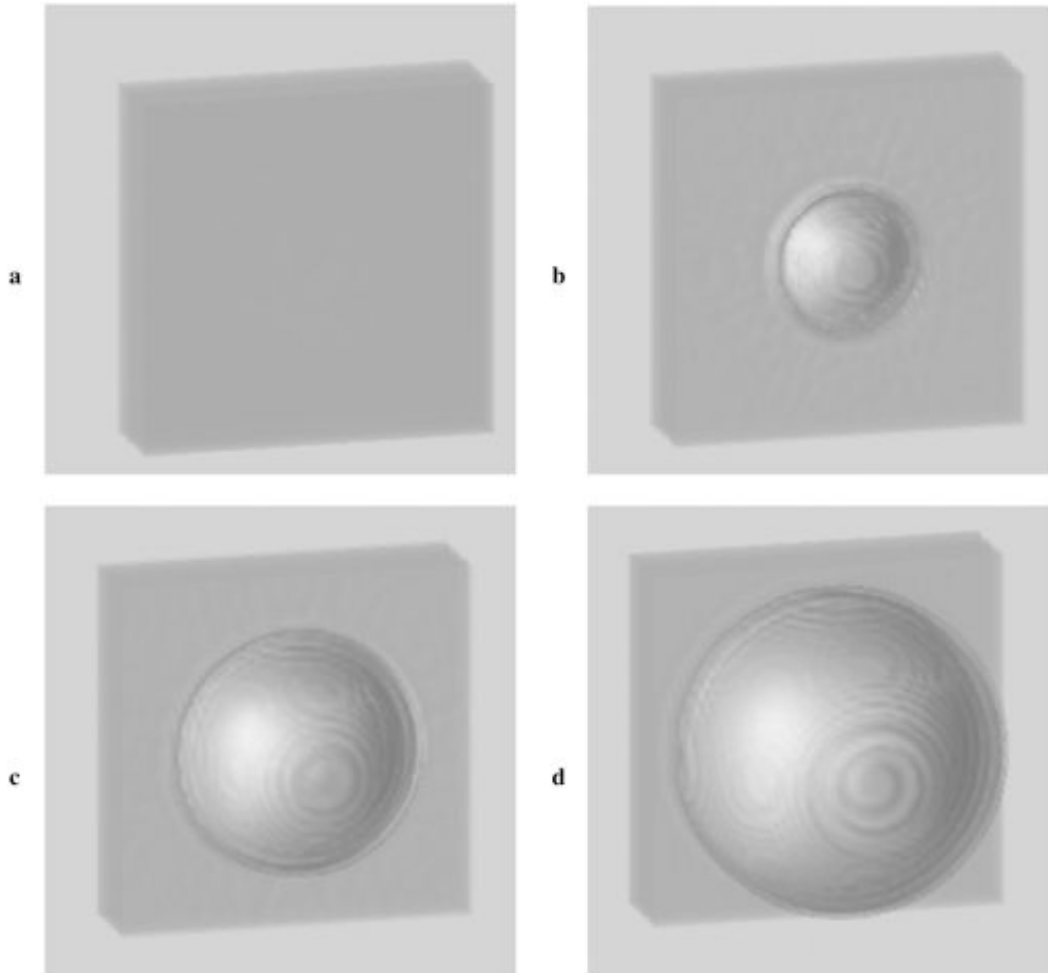


Fig. 8. Isosurface renderings of the total (logarithmically scaled) pressure wavefield associated with scattering from a “muscle” sphere of radius 1.5 mm. Incident pulse parameters were the same as in Fig. 4–6. Panels a–d show the wavefield at four instants separated by $0.79 \mu\text{s}$. The view shown is such that the incident wave is traveling into the page, so that the visible wavefield includes the backscattered component. The lowest amplitude isosurface shown is 67.5 dB down from the incident wave amplitude. Each panel shows a rendering of the entire computational domain (10.66 mm on each side). In panel a, the incident wavefront is just impinging on the sphere; in panel d, the scattered wavefront has just passed the computational boundary.

(PML) [38] can provide true radiation boundary conditions; however, present PML implementations are not applicable to the second-order wave equation employed here. Combination of a k -space method with PML boundary conditions may require derivation of a new k - t space time integrator for the first-order wave propagation equations.

The present derivation was based on the linear (small amplitude) acoustic propagation equations. The k -space method could be easily extended to incorporate finite amplitude acoustic effects. For example, the nonlinear terms of the Westervelt propagation equation (used in [33] for modeling of ultrasonic propagation in tissue) could be included as effective source terms additional to the effective sources v and q defined previously. The numerical results obtained suggest that the k -space method is most accurate when the effective source terms are fairly small; thus, a nonlinear extension to the k -space method should be highly accurate for weak nonlinear effects.

Computation times for the k -space method can be reduced easily by parallelization. The primary computa-

tional burden of the method is incurred in the multidimensional FFT taken at each time step. Because FFTs can be efficiently executed on parallel processors [24], [39], the present k -space method should scale efficiently to large problems that require parallel processing.

VI. CONCLUSIONS

A simplified derivation of the k -space method for computation of ultrasonic wave propagation has been presented. The method efficiently accounts for sound speed and density variations and can be extended to include realistic absorption effects and absorbing boundary conditions. Three-dimensional computations can also be performed without change to the algorithm as derived here.

Analytic and numerical results have shown that the present k -space method provides superior stability and accuracy over both a similar leapfrog pseudospectral method and a fourth-order space, second-order time, finite difference method. This improved accuracy allows larger spatial and time steps to be employed, so that large-scale multidimensional

mensional computations are more feasible. Computations using a realistic two-dimensional tissue model support the conclusion that the k -space method provides high accuracy and low computational cost for large-scale computations.

The results also indicate that care should be taken when choosing and implementing a forward solver for a particular scattering problem. For instance, in the present k -space method, one can suppress spurious waves by smoothing sound speed and density variations; however, this smoothing does not decrease the time-domain L^2 error in some cases. Similarly, the finite difference time-domain method employed here is less accurate than the k -space method in most cases examined here, but the method achieved higher accuracy for a test case with a bone-like scatterer. In general, the k -space method proposed here should be most applicable to large-scale scattering problems involving low contrast inhomogeneities, such as soft tissue structures.

ACKNOWLEDGMENT

The authors thank Fadil Santosa and Bengt Fornberg for helpful discussions.

REFERENCES

- [1] N. N. Bojarski, "The k -space formulation of the scattering problem in the time domain," *J. Acoust. Soc. Amer.*, vol. 72, no. 2, pp. 570–584, 1982.
- [2] —, "The k -space formulation of the scattering problem in the time domain: An improved single propagator formulation," *J. Acoust. Soc. Amer.*, vol. 77, no. 3, pp. 826–831, 1985.
- [3] B. Comani-Tabrizi, "K-space formulation of the absorptive full fluid elastic scalar wave equation in the time domain," *J. Acoust. Soc. Amer.*, vol. 79, no. 4, pp. 901–905, 1986.
- [4] S. Finette, "A computer model of acoustic wave scattering in soft tissue," *IEEE Trans. Biomed. Eng.*, vol. 34, no. 5, pp. 336–344, 1987.
- [5] S. Finette, "Computational methods for simulating ultrasound scattering in soft tissue," *IEEE Trans. Ultrason., Ferroelect., Freq. Contr.*, vol. 34, no. 3, pp. 283–292, 1987.
- [6] S. Pourjavid and O. J. Tretiak, "Numerical solution of the direct scattering problem through the transformed acoustical wave equation," *J. Acoust. Soc. Amer.*, vol. 91, no. 2, pp. 639–645, 1992.
- [7] Q. H. Liu, "Generalization of the k -space formulation to elastodynamic scattering problems," *J. Acoust. Soc. Amer.*, vol. 97, no. 3, pp. 1373–1379, 1995.
- [8] H.-O. Kreiss and J. Olinger, "Comparison of accurate methods for the integration of hyperbolic equations," *Tellus*, vol. 24, no. 3, pp. 199–215, 1972.
- [9] B. Fornberg, "On a Fourier method for the integration of hyperbolic," *SIAM J. Numer. Anal.*, vol. 12, no. 4, pp. 509–528, 1975.
- [10] D. Gottlieb and S. A. Orszag, *Numerical Analysis of Spectral Methods*. Philadelphia, PA: SIAM, 1977.
- [11] D. C. Witte and P. G. Richards, "The pseudospectral method for simulating wave propagation," in *Computational Acoustics*, vol. 3, D. Lee, A. Cakmak, and R. Vichnevetsky, Eds. New York: North-Holland, 1990, pp. 1–18.
- [12] B. Fornberg, "Introduction to PS method via finite differences," in *A Practical Guide to Pseudospectral Methods*. Cambridge: Cambridge University Press, 1996, ch. 3.
- [13] G. Wojcik, B. Fornberg, R. Waag, L. Carcione, J. Mould, L. Nikodym, and T. Driscoll, "Pseudospectral methods for large-scale bioacoustic models," in *Proc. IEEE Ultrason. Symp.*, 1997, vol. 2, pp. 1501–1506.
- [14] Q. H. Liu, "The pseudospectral time-domain (PSTD) algorithm for acoustic waves in absorptive media," *IEEE Trans. Ultrason., Ferroelect., Freq. Contr.*, vol. 45, no. 4, pp. 1044–1055, 1998.
- [15] A. D. Pierce, "The wave theory of sound," in *Acoustics: An Introduction to Its Physical Principles and Applications*, 2nd ed., Woodbury, NY: Acoustical Society of America, 1989, ch. 1.
- [16] S. A. Johnson and M. L. Tracy, "Inverse scattering solutions by a sinc basis moment method—Part I: Theory," *Ultrason. Imag.*, vol. 5, no. 4, pp. 361–375, 1983.
- [17] A. Nachman, "Reconstructions from boundary measurements," *Ann. Math.*, vol. 128, no. 3, pp. 531–576, 1988.
- [18] R. E. Mickens, *Nonstandard Finite Difference Models of Differential Equations*. Singapore: World Scientific, 1994.
- [19] B. Fornberg and G. B. Whitham, "A numerical and theoretical study of certain nonlinear wave phenomena," *Phil. Trans. R. Soc. London*, vol. 289, no. 1361, pp. 373–404, 1978.
- [20] E. H. Twizell, *Computational Methods for Partial Differential Equations*. New York: Ellis Horwood Limited, 1984.
- [21] E. Turkel, "On the practical use of high-order methods for hyperbolic systems," *J. Comp. Phys.*, vol. 35, no. 3, pp. 319–340, 1980.
- [22] R. E. Crochiere and L. R. Rabiner, *Multirate Digital Signal Processing*. Englewood Cliffs, NJ: Prentice-Hall, 1983.
- [23] T. D. Mast, L. M. Hinkelman, M. J. Orr, V. W. Sparrow, and R. C. Waag, "Simulation of ultrasonic pulse propagation through the abdominal wall," *J. Acoust. Soc. Amer.*, vol. 102, no. 2, pp. 1177–1190, 1998. [Erratum: *J. Acoust. Soc. Amer.*, vol. 104, no. 2, pp. 1124–1125, 1998.]
- [24] M. Frigo and S. G. Johnson, "FFTW: An adaptive software architecture for the FFT," in *Proc. of the ICASSP*, 1998, vol. 3, pp. 1381–1384.
- [25] R. W. MacCormack, "Numerical solution of the interaction of a shock wave with a laminar boundary layer," in *Lecture Notes in Physics*, vol. 8, J. Ehlers, K. Hepp, and H. A. Weidenmüller, Eds. Berlin: Springer-Verlag, 1971, pp. 151–163.
- [26] D. Gottlieb and A. Turkel, "Dissipative two-four methods for time-dependent problems," *Math. Comp.*, vol. 30, no. 136, pp. 703–723, 1976.
- [27] V. W. Sparrow and R. Raspet, "A numerical method for general finite amplitude wave propagation and its application to spark pulses," *J. Acoust. Soc. Amer.*, vol. 90, no. 5, pp. 2683–2691, 1991.
- [28] T. D. Mast, L. M. Hinkelman, M. J. Orr, and R. C. Waag, "Simulation of ultrasonic pulse propagation, distortion, and attenuation in the human chest wall," *J. Acoust. Soc. Amer.*, vol. 106, no. 6, pp. 3665–3677, 1999.
- [29] P. M. Morse and K. U. Ingard, "The scattering of sound," in *Theoretical Acoustics*. New York: McGraw-Hill, 1968, ch. 8.
- [30] A. V. Oppenheim and R. W. Schaffer, "Filter design techniques," in *Discrete-Time Signal Processing*, Englewood Cliffs, NJ: Prentice Hall, 1989, ch. 7.
- [31] R. L. Burden, J. D. Faires, and A. C. Reynolds, "Iterative techniques in matrix algebra," in *Numerical Analysis*. Boston, MA: Prindle, Weber, and Schmidt, 1978, ch. 8.
- [32] J. C. Mould, G. L. Wojcik, L. M. Carcione, M. Tabei, T. D. Mast, and R. C. Waag, "Validation of FFT-based algorithms for large-scale modeling of wave propagation in tissue," in *Proc. IEEE Ultrason. Symp.*, 1999, pp. 1551–1556.
- [33] I. M. Hallaj and R. O. Cleveland, "FDTD simulation of finite-amplitude pressure and temperature fields for biomedical ultrasound," *J. Acoust. Soc. Amer.*, vol. 105, no. 5, pp. L7–L12, 1999.
- [34] A. I. Nachman, J. Smith, and R. C. Waag, "An equation for acoustic propagation in inhomogeneous media with relaxation losses," *J. Acoust. Soc. Amer.*, vol. 88, no. 3, pp. 1584–1595, 1990.
- [35] X. Yuan, D. Borup, J. Wiskin, M. Berggren, and S. Johnson, "Simulation of acoustic wave propagation in dispersive media with relaxation losses by using FDTD method with PML absorbing boundary condition," *IEEE Trans. Ultrason., Ferroelect., Freq. Contr.*, vol. 46, no. 1, pp. 14–23, 1999.
- [36] T. L. Szabo, "Time domain wave equations for lossy media obeying a frequency power law," *J. Acoust. Soc. Amer.*, vol. 96, no. 1, pp. 491–500, 1994.
- [37] C. Cerjan, D. Kosloff, R. Kosloff, and M. Reshef, "A nonreflecting boundary condition for discrete acoustic and elastic wave equations," *Geophysics*, vol. 50, no. 4, pp. 705–708, 1985.
- [38] J.-P. Berenger, "A perfectly matched layer for the absorption of electromagnetic waves," *J. Comput. Phys.*, vol. 114, no. 2, pp. 185–200, 1994.

- [39] P. N. Swartztrauber, "Multiprocessor FFTs," *Parallel Computing*, vol. 5, no. 1, pp. 197–210, 1987.



T. Douglas Mast (M'98) was born in St. Louis, Missouri in 1965. He received a B.A. in physics and mathematics from Goshen College in 1987 and a Ph.D. in acoustics from The Pennsylvania State University in 1993. From 1993 until 1996, he was Postdoctoral Research Associate with the University of Rochester's Ultrasound Research Laboratory. Since 1996, he has been with the Applied Research Laboratory of The Pennsylvania State University, where he currently is Research Associate and Assistant Professor of Acoustics. His research

interests include propagation and scattering in inhomogeneous media, inverse scattering, tissue characterization, and nondestructive testing.



Laurent P. Souriau was born in Saint Maur, near Paris, France in 1964. He received the Engineer degree in physics from the Ecole Nationale Supérieure de Physique de Marseille in 1988 and the Ph.D. degree at the Université d'Orsay in 1996. He joined the Ultrasound Research Laboratory, the University of Rochester, Rochester, NY, as Research Associate in 1996. His research interests include submarine detection, biomedical acoustic imaging, and inverse problem theory.



D.-L. Donald Liu (M'93) obtained his Bachelor of Engineering degree in 1984 from the Department of Automatic Control, Qinghua University, Beijing, China and Master of Engineering degree and Doctor of Engineering degree in 1988 and 1991, respectively, both from the Department of Electronic Engineering, University of Tokyo, Tokyo, Japan. He was Assistant Professor in the Department of Electrical and Electronic Engineering at Sophia University, Tokyo, Japan from April 1991 to March 1992. From April 1992 to

March 1997, he was with the Department of Electrical Engineering at University of Rochester, Rochester, New York, where he was appointed Scientist and Assistant Professor. Since April 1997, he has been with Siemens Medical Systems, where he is currently Staff Systems Engineer. Dr. Liu's research interests include analysis and modeling of ultrasonic wavefront distortion, adaptive imaging through aberration correction, quantitative and 3-D ultrasonic imaging, spectral analysis, and digital signal processing.



Makoto Tabei (M'94) was born in Osaka, Japan in 1956. He received the B.E. degree in computer science from the University of Electro-Communications, Tokyo, Japan in 1979 and the M.E. and Dr.Eng. degrees in information processing from Tokyo Institute of Technology in 1981 and 1996, respectively. From 1981 to 1982, he was with Japan Atomic Energy Research Institute in Ibaraki, Japan, working as a research engineer. Since 1982, he has been Research Associate at the Precision and Intelligence Laboratory, Tokyo Institute of Technology. From 1989 to 1990, he was a visiting scientist at the Research Laboratory of Electronics of the Massachusetts Institute of Technology. He has been a visiting associate professor in the Department of Electrical and Computer Engineering, University of Rochester, since 1997. His research interests are in the areas of estimation theory, image reconstruction, and numerical analysis of acoustic wave propagation.



Adrian I. Nachman received his B.Sc. degree from McGill University in 1974 and the Ph.D. degree in mathematics from Princeton University in 1980. He was a J.W. Gibbs Instructor at Yale University from 1979 to 1981. In 1981, he joined the faculty of the University of Rochester, where he is now Professor in the Department of Mathematics. Dr. Nachman's recent research has involved the development of new nonlinear reconstruction methods for electric impedance imaging and other boundary value problems in two and three dimensions, multidimensional inverse scattering problems, and quantitative ultrasonic imaging. He is a member of the Society for Industrial and Applied Mathematics.

Department of Electrical Engineering, School of Engineering and Applied Science and also holds an appointment in the Department of Radiology, School of Medicine and Dentistry. Prof. Waag's recent research has treated ultrasonic scattering, propagation, and imaging in medical applications. In 1992, he received the Joseph H. Holmes Pioneer Award from the American Institute of Ultrasound in Medicine. He is a Fellow of the Institute of Electrical and Electronics Engineers, the Acoustical Society of America, and the American Institute of Ultrasound in Medicine.



Robert C. Waag (S'59–M'66–SM'83–F'90) received his B.E.E., M.S., and Ph.D. degrees from Cornell University in 1961, 1963, and 1965, respectively. After completing his Ph.D. studies, he became a member of the technical staff at Sandia Laboratories, Albuquerque, NM and then served as an officer in the United States Air Force from 1966 to 1969 at the Rome Air Development Center, Griffiss Air Force Base, NY. In 1969, he joined the faculty of the University of Rochester, where he is now Arthur Gould Yates Professor in the

Department of Electrical Engineering, School of Engineering and Applied Science and also holds an appointment in the Department of Radiology, School of Medicine and Dentistry. Prof. Waag's recent research has treated ultrasonic scattering, propagation, and imaging in medical applications. In 1992, he received the Joseph H. Holmes Pioneer Award from the American Institute of Ultrasound in Medicine. He is a Fellow of the Institute of Electrical and Electronics Engineers, the Acoustical Society of America, and the American Institute of Ultrasound in Medicine.